Experimental realization of a programmable quantum gate

Michal Mičuda, Miroslav Ježek, Miloslav Dušek, and Jaromír Fiurášek
Department of Optics, Palacký University, 17. lstopadu 50, 77200 Olomouc, Czech Republic
(Received 16 June 2008; published 5 December 2008)

We experimentally demonstrate a programmable single-qubit quantum gate. This device applies a unitary phase shift operation to a data qubit with the value of the phase shift being fully determined by the state of a program qubit. Our linear optical implementation is based on the encoding of qubits into polarization states of single photons, two-photon interference on a polarizing beam splitter, and measurement on the output program qubit. We fully characterize the programmable gate by quantum process tomography. The achieved average quantum process fidelity exceeding 97% illustrates very good performance of the gate for all values of the encoded phase shift. We also show that by using a different set of program states the device can operate as a programmable partial polarization filter.

DOI: 10.1103/PhysRevA.78.062311 PACS number(s): 03.67.−a, 42.50.Ex

Classical computers rely on the combination of a fixed hardware and a flexible software. The operation performed on the data register is fully determined by the information stored in the program register and can be altered at will by the user. It is intriguing to attempt to generalize this concept to quantum computing [1]. Imagine a fixed universal quantum processing unit where the transformation of the data qubits is specified by the quantum state of program qubits. In a seminal paper [2] Nielsen and Chuang proved that an n qubit quantum register can perfectly encode at most 2^n distinct quantum operations. Since already unitary transformations on a single qubit form the SU(2) group with uncountably many elements, this bound seems to severely limit the universality of programmable quantum gates.

Although perfect universal programmability is ruled out, it is nevertheless possible to construct approximate programmable quantum gates and optimize their performance for a given size of the program register [3–8]. Two complementary approaches to this problem were pursued in the literature. One option is to design gates that operate deterministically, i.e., always provide an output, but add some noise to the output state [8]. An alternative strategy avoids the extra noise at a cost of reduced success probability [2–4]. The gate then involves a measurement whose outcome heralds its success or failure. If restricted to successful cases, the gate operates perfectly and noiselessly.

A very important elementary programmable quantum gate was proposed by Vidal, Masanes, and Cirac (VMC) [3]. They considered programmable rotation of a single qubit along the z axis of the Bloch sphere,

$$U(\phi) = |0\rangle\langle 0| + e^{i\phi}|1\rangle\langle 1|. \tag{1}$$

Here $|0\rangle$ and $|1\rangle$ denote the computational basis states of the qubit. In the simplest version of VMC protocol, the phase shift ϕ is encoded into a state of single-qubit program register,

$$|\phi\rangle_P = \frac{1}{\sqrt{2}}(|0\rangle + e^{i\phi}|1\rangle). \tag{2}$$

A controlled-NOT (CNOT) gate is applied to the data qubit $|\psi\rangle_D = \alpha|0\rangle + \beta|1\rangle$ and the program qubit $|\phi\rangle_P$. This is followed by measurement on the program qubit in the computational basis. The measurement outcome $|0\rangle$ indicates successful application of $U(\phi)$ onto the data qubit while the outcome $|1\rangle$ means that the operation $U(-\phi)$ has been applied. This scheme thus exhibits a success probability of 50% which is the maximum possible with a single–qubit program register. By adding further program qubits, the probability of success can be made arbitrary close to unity. Note that an exact specification of the phase shift ϕ would require infinitely many classical bits. A striking feature of the programmable quantum gate is that the information on ϕ is faithfully encoded into *a single* quantum bit.

While the theory of programmable quantum gates is well established, little attention has been paid to their experimental realizations. The single-qubit programmable quantum measurement devices [9–18], where the state of the program qubit determines the measurement on the data qubit, were implemented for single photons [19] and for nuclear spins in a nuclear magnetic resonance experiment [20]. Also a programmable discriminator of coherent states has been reported [21,22]. However, to our knowledge, there is no demonstration of a programmable unitary quantum gate for photonic qubits. In this paper we close this gap between theory and experiment. Specifically, we implement the elementary single-qubit programmable gate proposed by VMC [3].

Our optical implementation is based on the encoding of qubits into polarization states of single photons. We exploit two-photon interference on a polarizing beam splitter (PBS). Consider the input states of data and program photons,

$$|\psi\rangle_D = \alpha|H\rangle + \beta|V\rangle, \quad |\phi\rangle_P = \frac{1}{\sqrt{2}}(|H\rangle + e^{i\phi}|V\rangle), \tag{3}$$

where $|H\rangle$ and $|V\rangle$ denote the horizontal and vertical linear polarization states, respectively. Suppose that the PBS totally transmits horizontally polarized photons and reflects vertically polarized photons. If we restrict ourselves to the cases when a single photon emerges in each output port of the PBS [23–25], then the conditional two-photon output state reads

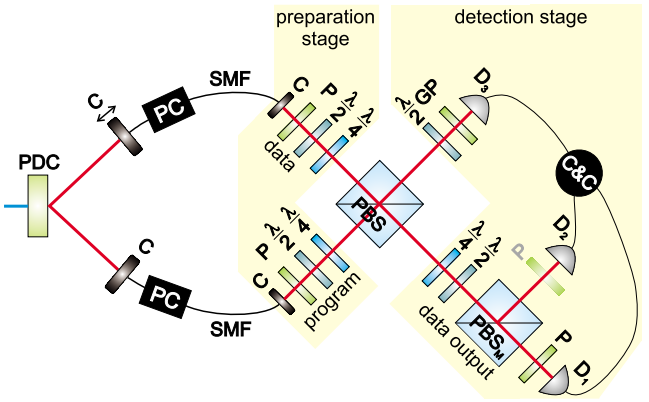

FIG. 1. (Color online) Scheme of the experimental setup. The correlated photons generated in the process of spontaneous parametric down conversion (PDC) serve as the program and data qubits. After being prepared in proper polarization states the photons interfere on the PBS. The detection stage consists of polarization analysis, single-photon detectors (D), and coincidence logic and counting module ($C\&C$). For polarization setting and analysis the fiber polarization controllers (PCs), half-wave plates ($\frac{\lambda}{2}$), quarter-wave plates ($\frac{\lambda}{4}$), linear film polarizers (P), Glan polarizer (GP), and polarizing beam splitter ($\mathrm{PBS_M}$) are used. See text for details.

$$\frac{1}{\sqrt{2}}(\alpha|H\rangle_D|H\rangle_P + \beta e^{i\phi}|V\rangle_D|V\rangle_P). \tag{4}$$

If the program qubit is measured in the diagonal linear polarization basis $|\pm\rangle = \frac{1}{\sqrt{2}}(|H\rangle \pm |V\rangle)$ then the data qubit is prepared according to the measurement result in the state

$$|\psi_{\mathrm{out}}\rangle_D = \alpha|H\rangle \pm \beta e^{i\phi}|V\rangle. \tag{5}$$

If the measurement outcome is $|+\rangle$ then the unitary transformation $U(\phi)$ has been applied to the data photon. If the outcome is $|-\rangle$ then the complex amplitude of state $|V\rangle$ acquires an extra relative π phase shift with respect to the amplitude of the state $|H\rangle$. This can be compensated by a fast electro-optical modulator that applies a relative phase shift 0 or π depending on the measurement outcome [26,27]. With the active feed forward the scheme achieves the success probability 50%. This saturates the bound on the achievable success probability [3] so this linear optical scheme is optimal. In the experiment we implemented a passive version of the scheme without feed forward. We postselect only the events when the program qubit is projected onto state $|+\rangle$ which reduces the theoretical success probability of the protocol to 25%.

The experimental setup is shown in Fig. 1. The initial pump beam from a continuous-wave laser (CUBE 405 C, Coherent) with the wavelength of 407 nm is focused to 6 mm thick nonlinear crystal $LiIO_3$ cut for type-I degenerate spontaneous parametric down conversion (PDC). After filtering out the scattered pump light by cutoff filters the down-converted photon pairs with a wavelength of 814 nm are coupled (C) into single-mode optical fibers (SMFs) acting as spatial filters. The photons are prepared in a horizontal polarization state at the fibers' outputs by fiber polarization controllers (PCs). To achieve maximal polarization purity two linear film polarizers (P) are employed. The required polarization states of both the data and program photons are set in the preparation stage by properly rotated wave plates ($\frac{\lambda}{2}$, $\frac{\lambda}{4}$). The data and program photons interfere on the polarizing beam splitter (PBS, Ekspla) and enter the detection stage. The data photon passes through a sequence of a quarter-wave plate, a half-wave plate, and another polarizing beam splitter, $\mathrm{PBS_M}$, which allows one to measure the photon in an arbitrary polarization basis. The program photon is projected onto the diagonal linearly polarized state $|+\rangle$ by a half-wave plate and a calcite Glan polarizer (GP). At the outputs the photons are detected by fiber-coupled single-photon avalanche photodiodes (APD; SPCM-AQ4C, Perkin Elmer). Detection events registered by the detectors D_1, D_2, and D_3 are processed by coincidence logic (TAC/SCA, Ortec) and fed into a counting module (Ortec).

To verify the overlap of photons' spatial mode functions on the PBS we measure the visibility of the Hong-Ou-Mandel (HOM) dip [28] in the data output port. The data and program photons are prepared in horizontal and vertical polarization states, respectively, so that they both propagate to the data output. The wave plates in the data detection stage are set to transform the H and V linear polarizations onto the diagonal ones. The HOM dip in coincidences between clicks of detectors D_1 and D_2 is measured as a function of the time delay between the program and data photons introduced by a motorized translation of one of the fiber coupling systems. The measured HOM dip visibility is above 89%, limited mainly by imperfections of $\mathrm{PBS_M}$. Particularly, if we insert two linear film polarizers in front of APDs D_1 and D_2 the visibility exceeds 99.5%. This indicates nearly perfect spatial overlap of the data and program photons on the PBS. The linear film polarizer placed before detector D_2 is removed in further measurements and used in the state preparation stage to ensure preparation of a pure input state.

The success of the gate is heralded by a coincidence detection of a single photon in each output port. In the experiment, we therefore measure the coincidence rates C_{13} between detectors D_1 and D_3 and C_{23} between detectors D_2 and D_3. The width of the coincidence window is set to 2 ns. For a given phase shift ϕ we characterize the performance of the programmable gate by a tomographically complete measurement. We set the state of the program photon to $\frac{1}{\sqrt{2}}(|H\rangle + e^{i\phi}|V\rangle)$. We then subsequently prepare the data photon in six different states $|H\rangle$, $|V\rangle$, $|+\rangle$, $|-\rangle$, $|R\rangle$, and $|L\rangle$, where $|R\rangle = \frac{1}{\sqrt{2}}(|H\rangle + i|V\rangle)$ and $|L\rangle = \frac{1}{\sqrt{2}}(|H\rangle - i|V\rangle)$ denote the right and left circularly polarized states, respectively. For each input we carry out measurements for six different settings of the wave plates in the data detection stage chosen such that the click of D_1 heralds projection of the data photon onto the state $|H\rangle$, $|V\rangle$, $|+\rangle$, $|-\rangle$, $|R\rangle$, and $|L\rangle$ by turns. Every particular measurement takes 5 s and is repeated ten times to gain statistics. The average twofold coincidence rate is about 1300 $\mathrm{s^{-1}}$. The polarizer placed in front of the detector D_1 guarantees nearly ideal projection onto a pure polarization state. Therefore, the presented results were obtained using only C_{13} coincidence data. Note that in this way we do not need to precisely calibrate the relative detection efficiencies of D_1 and D_2. We have confirmed that the results remain

largely unchanged if we use the coincidences C_{23} instead or if we process all data simultaneously. However, the results obtained from C_{23} exhibit slightly higher noise due to imperfect polarization filtering by the polarizing beam splitter, $\mathrm{PBS}_{\mathrm{M}}$ [29].

From the experimental data we reconstruct the completely positive (CP) map that fully characterizes the transformation of the data photon for a fixed state of the program photon. We have performed the quantum process tomography for eight different phase shifts $\phi=\frac{k}{4}\pi$, $k=0,1,\ldots,7$. According to the Jamiolkowski-Choi isomorphism [30,31], every CP map can be represented by a positive semidefinite operator χ on the tensor product of the input and output Hilbert spaces $\mathcal{H}_{\mathrm{in}}$ and $\mathcal{H}_{\mathrm{out}}$. In our case both $\mathcal{H}_{\mathrm{in}}$ and $\mathcal{H}_{\mathrm{out}}$ are two-dimensional Hilbert spaces of the polarization state of a single photon hence χ is a 4×4 matrix. The input state ρ_{in} transforms according to the formula

$$\rho_{\mathrm{out}}=\mathrm{Tr}_{\mathrm{in}}[(\rho_{\mathrm{in}}^{T}\otimes\mathbb{1}_{\mathrm{out}})\chi],$$

where T denotes transposition in a fixed basis. Due to the slight imperfections of the PBS, the implemented operation is not exactly unitary and may involve some polarization filtering. We therefore do not impose the constraint that χ has to be trace preserving but allow for a general trace-decreasing map [32,33]. We use the iterative maximum-likelihood estimation algorithm that is described in detail elsewhere [34,35]. This statistical reconstruction method yields a quantum process χ that is most likely to produce the observed experimental data [36,37].

Figure 2 displays the real and imaginary parts of the reconstructed CP map χ for four different phase shifts $\phi=k\frac{\pi}{2}$, $k=0,1,2,3$. We quantify the gate performance by the process fidelity defined as follows:

$$F_{\chi}=\frac{\mathrm{Tr}[\chi\chi_{\mathrm{id}}(\phi)]}{\mathrm{Tr}[\chi]\mathrm{Tr}[\chi_{\mathrm{id}}(\phi)]}. \tag{6}$$

Here $\chi_{\mathrm{id}}(\phi)$ is a process matrix representing the unitary operation $U(\phi)$ (1),

$$\chi_{\mathrm{id}}(\phi)=\mathbb{1}\otimes U(\phi)|\Phi^{+}\rangle\langle\Phi^{+}|\mathbb{1}\otimes U^{\dagger}(\phi), \tag{7}$$

where $|\Phi^{+}\rangle=|H\rangle|H\rangle+|V\rangle|V\rangle$ denotes the maximally entangled Bell state. Thus χ_{id} is effectively a density matrix of a pure maximally entangled state on $\mathcal{H}_{\mathrm{in}}\otimes\mathcal{H}_{\mathrm{out}}$. The process fidelity determined from the reconstructed CP maps is plotted in Fig. 3 as a function of the phase shift ϕ. We can see that the fidelity is almost constant and exceeds 95% for all values of ϕ which demonstrates very good functionality of the programmable gate.

A careful analysis of the reconstructed CP maps reveals that the PBS imposes a certain nonzero relative phase shift $\delta\phi$ between the vertical and horizontal polarizations. The active area of the PBS where splitting of the vertical and horizontal polarization components occurs is made of a stack of thin dielectric films. In principle, each of the polarization and spatial modes passing through the PBS can acquire a different phase shift. However, only a single effective combination of such phase shifts is relevant in our experiment and gives rise to the phase offset $\delta\phi$.

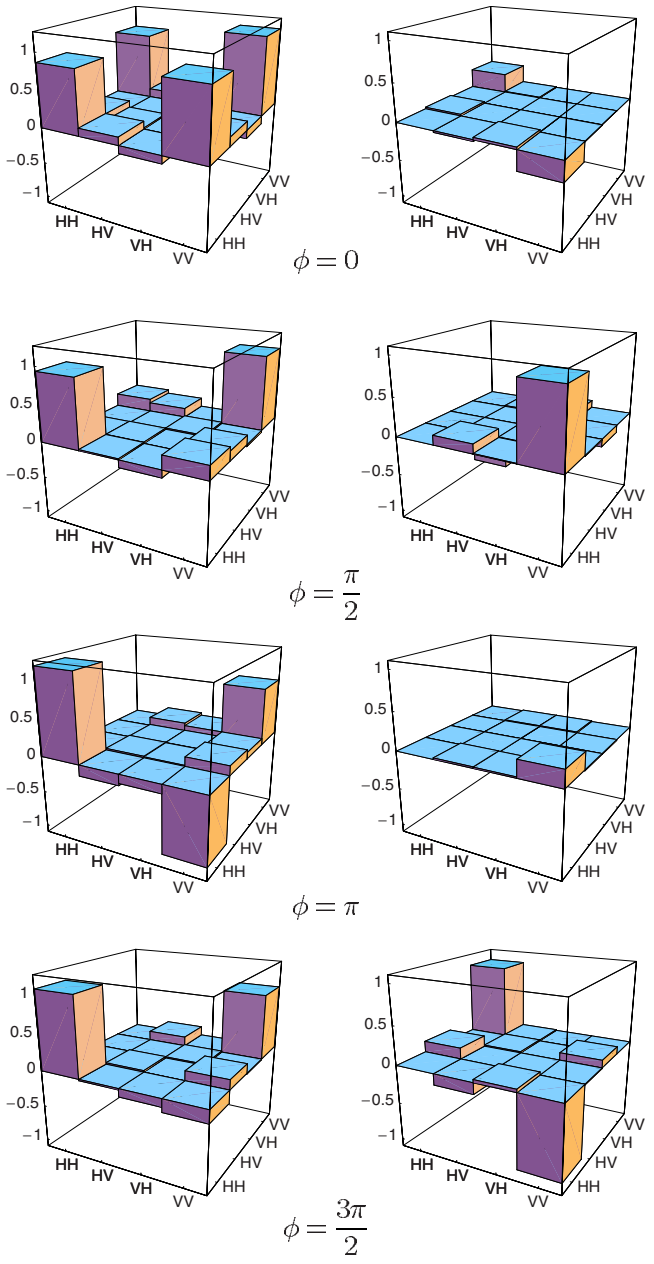

FIG. 2. (Color online) Reconstructed process matrix χ. Real (left column) and imaginary (right column) parts of the reconstructed CP map χ are shown for four different values of the programmed phase shift ϕ encoded in the state of the program photon.

We estimate the phase offset as follows. For each value of the encoded phase shift ϕ we determine the effective applied phase shift ϕ_{eff} by maximizing the overlap $\mathrm{Tr}[\chi\chi_{\mathrm{id}}(\phi_{\mathrm{eff}})]$ over ϕ_{eff}. The dependence of ϕ_{eff} on ϕ is plotted in Fig. 4. From the best linear fit to the data we obtain $\delta\phi=-0.265$ rad. This phase offset could be passively compensated, e.g., by means of additional wave plates that would apply the relative phase shift $-\delta\phi$ to the output data photon. We have carried out the software compensation and corrected the reconstructed CP maps for the fixed phase offset. This calibration procedure increases the process fidelity by about 1% as shown in Fig. 3. All the compensated fidelity data are within one percent around the average value of

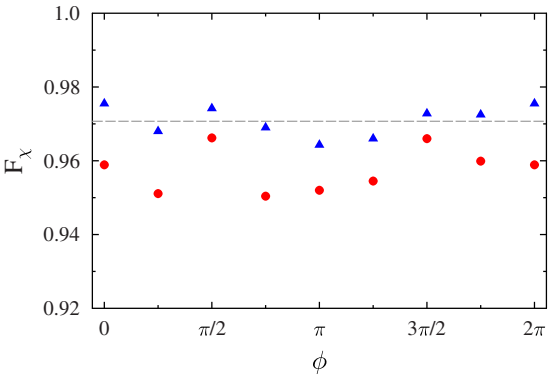

FIG. 3. (Color online) Quantum process fidelity of the programmable gate is plotted as a function of the encoded phase shift ϕ. The fidelities before (●) and after (▲) compensation of the constant phase offset $\delta\phi$ are shown. The dashed line represents the best constant fit to the compensated fidelity data with the value of 97.1%.

97.1%. The achievable gate fidelity is mainly limited by the imperfections of the PBS that does not totally reflect (transmit) the V (H) polarization. The measured splitting ratios read 97.7:2.3 and 0.5:99.5 for vertical and horizontal polarizations, respectively. A simple theoretical model predicts average process fidelity 97.4% which is in very good agreement with the experimental results.

Besides the quantum processes we have also reconstructed the single-qubit output state for each input state. We have evaluated the state fidelity $F=\langle\psi_{\text{out}}|\rho|\psi_{\text{out}}\rangle$ between the expected pure output state and the reconstructed (generally mixed) state ρ. For each phase shift ϕ we average the state fidelity over the six different input states to obtain the average state fidelity F_{av}. We find that F_{av} lies in the interval 96.6%–97.8%. The compensation of the phase offset $\delta\phi$ increases the average state fidelity by almost 1% to the range 97.6%–98.5%. This further confirms that the programmable gate operates with very high fidelity for all values of the phase shift ϕ in the interval $[0,2\pi]$.

The average state fidelity F_{av} and the process fidelity F_χ exhibit almost perfect linear dependence of the form $F_{\text{av}}=0.727F_\chi+0.275$. This is consistent with the theoretically

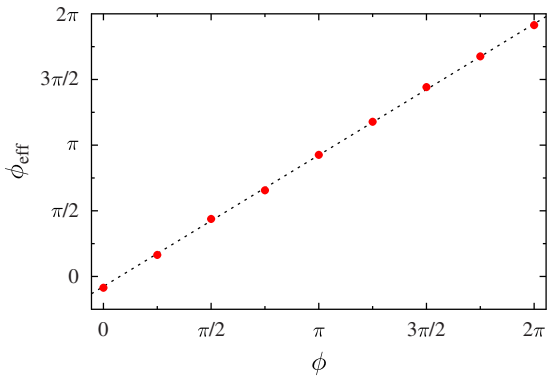

FIG. 4. (Color online) Dependence of the effectively applied phase shift ϕ_{eff} on the programmed phase shift ϕ. The circles represent results obtained from the reconstructed CP maps; the dashed line is the best linear fit to the data.

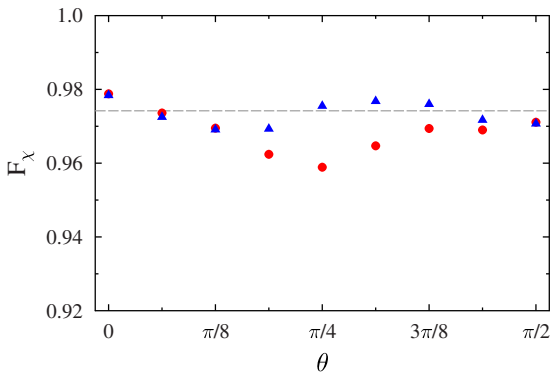

FIG. 5. (Color online) Quantum process fidelity of the programmable partial polarization filter is plotted as a function of the filtering angle θ. The fidelities before (●) and after (▲) compensation of the constant phase offset $\delta\phi$ are shown. The dashed line represents the best constant fit to the compensated fidelity data with the value of 97.4%.

predicted relation between these two fidelities for deterministic processes [38], $F_{\text{av}}=\frac{1}{3}(2F_\chi+1)$. The observed discrepancy is mainly due to the fact that we perform independent maximum likelihood reconstructions of the quantum process and output states while the theoretical formula assumes that the output states are calculated from the input states using the process matrix χ. Also, the reconstructed CP map is not exactly trace preserving.

We next show that our device can also function as a programmable partial polarization filter [6]. For this purpose we prepare the program qubit in various linear polarization states $\cos\theta|H\rangle+\sin\theta|V\rangle$. Repeating the calculation leading to Eq. (5) we find the (non-normalized) output state of the data qubit to be

$$|\psi_{\text{out}}\rangle_D=\alpha\cos\theta|H\rangle+\beta\sin\theta|V\rangle. \tag{8}$$

The amplitude of vertical polarization is attenuated (or amplified) by a factor of $\tan\theta$ with respect to the amplitude of the horizontal polarization. We carry out the complete quantum process tomography of the programmable quantum filter for nine different values of $\theta=\frac{n}{16}\pi$, $n=0,1,\ldots,8$. The process fidelity can be calculated according to Eq. (6) where the ideal filtering operation is now described by a partially entangled state,

$$\chi_{\text{id,filter}}(\theta)=(\cos\theta|H\rangle|H\rangle+\sin\theta|V\rangle|V\rangle)(\langle H|\langle H|\cos\theta + \langle V|\langle V|\sin\theta).$$

The experimentally determined process fidelity is plotted in Fig. 5. Similarly as for the programmable unitary gate, the compensation of the constant phase offset $\delta\phi$ increases the fidelity. The improvement is most significant for $\theta=\pi/4$ while for complete filtering ($\theta=0$ and $\theta=\pi/2$) the phase shift is irrelevant and its compensation does not change the fidelity.

In conclusion, the programmable single-qubit phase gate working on single-photon polarization-encoded qubits has been proposed and experimentally developed. The gate op-

eration has been thoroughly tested by complete quantum process tomography. The comparison of the reconstructed processes and the corresponding theoretical ones yields high process fidelity of about 97% with negligible dependence on the encoded phase shift. It has been demonstrated that with a different set of program states, the device can also operate as a programmable partial polarization filter. The implemented programmable gates can serve as building blocks of more complex multiqubit linear-optics quantum gates or other optical quantum information processing devices.

We would like to thank Lucie Bartůšková for help and fruitful discussions during the experiment. This work has been supported by Research Projects "Center of Modern Optics" (Contract No. LC06007) and "Measurement and Information in Optics" (Contract No. MSM 6198959213) of the Czech Ministry of Education.

[1] M. A. Nielsen and I. L. Chuang, *Quantum Computation and Quantum Information* (Cambridge University Press, Cambridge, 2000).
[2] M. A. Nielsen and I. L. Chuang, Phys. Rev. Lett. **79**, 321 (1997).
[3] G. Vidal, L. Masanes, and J. I. Cirac, Phys. Rev. Lett. **88**, 047905 (2002).
[4] M. Hillery, V. Bužek, and M. Ziman, Phys. Rev. A **65**, 022301 (2002).
[5] M. Hillery, M. Ziman, and V. Bužek, Phys. Rev. A **66**, 042302 (2002).
[6] M. Hillery, M. Ziman, and V. Bužek, Phys. Rev. A **69**, 042311 (2004).
[7] A. Brazier, V. Bužek, and P. L. Knight, Phys. Rev. A **71**, 032306 (2005).
[8] M. Hillery, M. Ziman, and V. Bužek, Phys. Rev. A **73**, 022345 (2006).
[9] G. M. D'Ariano and P. Perinotti, Phys. Rev. Lett. **94**, 090401 (2005).
[10] S. M. Barnett, A. Chefles, and I. Jex, Phys. Lett. A **307**, 189 (2003).
[11] G. M. D'Ariano, P. Perinotti, and M. F. Sacchi, Europhys. Lett. **65**, 165 (2004).
[12] M. Dušek and V. Bužek, Phys. Rev. A **66**, 022112 (2002).
[13] J. Fiurášek, M. Dušek, and R. Filip, Phys. Rev. Lett. **89**, 190401 (2002).
[14] J. Fiurášek and M. Dušek, Phys. Rev. A **69**, 032302 (2004).
[15] J. A. Bergou and M. Hillery, Phys. Rev. Lett. **94**, 160501 (2005).
[16] B. He and J. A. Bergou, Phys. Rev. A **75**, 032316 (2007).
[17] C. Zhang, M. Ying, and B. Qiao, Phys. Rev. A **74**, 042308 (2006).
[18] J. A. Bergou, V. Bužek, E. Feldman, U. Herzog, and M. Hillery, Phys. Rev. A **73**, 062334 (2006).
[19] J. Soubusta, A. Černoch, J. Fiurášek, and M. Dušek, Phys. Rev. A **69**, 052321 (2004).
[20] T. Gopinath, R. Das, and A. Kumar, Phys. Rev. A **71**, 042307 (2005).
[21] M. Sedlák, M. Ziman, O. Přibyla, V. Bužek, and M. Hillery, Phys. Rev. A **76**, 022326 (2007).
[22] L. Bartůšková, A. Černoch, J. Soubusta, and M. Dušek, Phys. Rev. A **77**, 034306 (2008).
[23] T. B. Pittman, B. C. Jacobs, and J. D. Franson, Phys. Rev. A **64**, 062311 (2001).
[24] T. B. Pittman, B. C. Jacobs, and J. D. Franson, Phys. Rev. Lett. **88**, 257902 (2002).
[25] T. B. Pittman, M. J. Fitch, B. C. Jacobs, and J. D. Franson, Phys. Rev. A **68**, 032316 (2003).
[26] F. Sciarrino, M. Ricci, F. De Martini, R. Filip, and L. Mišta, Jr., Phys. Rev. Lett. **96**, 020408 (2006).
[27] R. Prevedel, P. Walther, F. Tiefenbacher, P. Bohl, R. Kaltenbaek, T. Jennewein, and A. Zeilinger, Nature (London) **445**, 65 (2007).
[28] C. K. Hong, Z. Y. Ou, and L. Mandel, Phys. Rev. Lett. **59**, 2044 (1987).
[29] The process and state fidelities determined using coincidences C_{23} are about 1% lower than the fidelities obtained from coincidences C_{13}.
[30] A. Jamiołkowski, Rep. Math. Phys. **3**, 275 (1972).
[31] M.-D. Choi, Linear Algebr. Appl. **10**, 285 (1975).
[32] A. Černoch, L. Bartůšková, J. Soubusta, M. Ježek, J. Fiurášek, and M. Dušek, Phys. Rev. A **74**, 042327 (2006).
[33] A. Černoch, J. Soubusta, L. Bartůšková, M. Dušek, and J. Fiurášek, Phys. Rev. Lett. **100**, 180501 (2008).
[34] M. Ježek, J. Fiurášek, and Z. Hradil, Phys. Rev. A **68**, 012305 (2003).
[35] Z. Hradil, J. Řeháček, J. Fiurášek, and M. Ježek, Lect. Notes Phys. **649**, 59 (2004).
[36] Z. Hradil, Phys. Rev. A **55**, R1561 (1997).
[37] K. Banaszek, G. M. D'Ariano, M. G. A. Paris, and M. F. Sacchi, Phys. Rev. A **61**, 010304(R) (1999).
[38] M. Horodecki, P. Horodecki, and R. Horodecki, Phys. Rev. A **60**, 1888 (1999).